

A Homotetrameric Kinesin-5, KLP61F, Bundles Microtubules and Antagonizes Ncd in Motility Assays

Li Tao,¹ Alex Mogilner,¹ Gul Civelekoglu-Scholey,¹ Roy Wollman,¹ James Evans,² Henning Stahlberg,² and Jonathan M. Scholey^{1,2,*}

¹Laboratory of Cell and Computational Biology
Center for Genetics and Development
University of California, Davis
Davis, California 95616

²Section of Molecular and Cellular Biology
University of California, Davis
Davis, California 95616

Summary

Background: Mitosis depends upon the cooperative action of multiple microtubule (MT)-based motors. Among these, a kinesin-5, KLP61F, and the kinesin-14, Ncd, are proposed to generate antagonistic-sliding forces that control the spacing of the spindle poles. We tested whether purified KLP61F homotetramers and Ncd homodimers can generate a force balance capable of maintaining a constant spindle length in *Drosophila* embryos. **Results:** Using fluorescence microscopy and cryo-EM, we observed that purified full-length, motorless, and tailless KLP61F tetramers (containing a tetramerization domain) and Ncd dimers can all cross-link MTs into bundles in MgATP. In multiple-motor motility assays, KLP61F and Ncd drive plus-end and minus-end MT sliding at 0.04 and 0.1 $\mu\text{m/s}$, respectively, but the motility of either motor is decreased by increasing the mole fraction of the other. At the “balance point,” the mean velocity was zero and MTs paused briefly and then oscillated, taking $\sim 0.3 \mu\text{m}$ excursions at $\sim 0.02 \mu\text{m/s}$ toward the MT plus end and then the minus end. **Conclusions:** The results, combined with quantitative analysis, suggest that these motors could act as mutual brakes to modulate the rate of pole-pole separation and could maintain a prometaphase spindle displaying small fluctuations in its steady-state length.

Introduction

Members of the kinesin-5 family of microtubule (MT) motors [1] play critical roles in mitosis [2–8], and their importance is underscored by the finding that yeast cell division and viability can be supported by a kinesin-5, Cin8p, plus one other factor, a MT depolymerase [3]. In *Drosophila melanogaster* embryos, genetic experiments and antibody-inhibition experiments suggest that a kinesin-5, KLP61F, is required to maintain the bipolar prometaphase spindle [5, 9, 10]. During metaphase and anaphase, KLP61F is proposed to drive the persistent outward sliding of interpolar (ip) MTs; this outward sliding not only drives anaphase B spindle elongation, but also, when coupled to ipMT depolymerization at

spindle poles, underlies poleward flux [11, 12]. Studies in frog extracts support the latter model for kinesin-5 action [13–15].

Native KLP61F purified via MT affinity from *Drosophila* embryos has a homotetrameric, bipolar structure, formed by the antiparallel arrangement of kinesin-related motor subunits, with pairs of motor domains at opposite ends of a single rod [2, 16, 17], and a similar architecture was subsequently proposed for frog and yeast kinesin-5 [18, 19]. Because kinesin-5 motors drive slow, plus-end-directed MT motility [2, 7, 19, 20], it is plausible that kinesin-5 functions by cross-linking and sliding apart antiparallel ipMTs in a “sliding filament” mechanism. In support of this hypothesis, kinesin-5 forms cross-bridges between ipMTs in the spindle interzone [21] and slides apart antiparallel MTs in motility assays [19]. This can be controlled by the phosphorylation of the bimC box within the kinesin-5 tail; this phosphorylation targets the protein to its site of action within the spindle [21, 22].

In many systems, the action of kinesin-5 motors is antagonized by the minus-end-directed, homodimeric kinesin-14 motors, which are capable of bundling MTs in vitro [23–27]. In *Drosophila* embryos, for example, antibody inhibition of KLP61F in null mutants lacking Ncd, a kinesin-14, suggests that Ncd drives an inward sliding of ipMTs that antagonizes KLP61F [9, 10]. Thus a balance of forces exerted on the spindle poles by KLP61F-generated outward ipMT sliding and Ncd-generated inward ipMT sliding is proposed to maintain the prometaphase spindle at a constant, steady-state length [9, 10, 28].

In vitro motility assays using small numbers of motors reveal that Ncd is a relatively fast (0.1 $\mu\text{m/s}$), nonprocessive, low-duty-ratio mitotic motor, capable of generating pN-scale stall forces, so that a critical number of motors is necessary to ensure that at least one motor is in a strong binding state at all times to slide ipMTs [26, 29, 30]. The kinesin-5 motor Eg5, on the other hand, is a slower (0.01–0.04 $\mu\text{m/s}$) processive motor characterized by almost linear force-velocity relations for hindering loads of up to 4 pN, with higher loads serving to detach the motor from its track [20].

In fly-embryo spindles, multiple KLP61F and Ncd motors are thought to act collectively and antagonistically, but it is unclear how “collective antagonism” would influence individual motor output or whether it could produce the predicted stable steady-state spindle length [9]. To our knowledge, competitive motility assays with antagonistic, opposite-polarity motors have only been performed previously with small numbers of kinesin-1 and dynein [31], where the alternating action of the two transport motors caused MTs to undergo bidirectional plus- and minus-end-directed motion, but it is unclear whether similar motility would be driven by other antagonistic motors, like KLP61F and Ncd, that act in large numbers in the spindle.

Competitive in vitro motility assays could reveal the type of motility driven by the composite action of

*Correspondence: jmscholey@ucdavis.edu

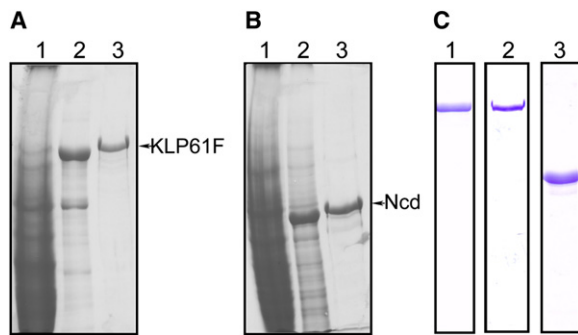


Figure 1. Purification of Recombinant KLP61F and Ncd from the Baculovirus Expression System

Commasie-blue-stained SDS-polyacrylamide gels show typical recombinant-motor-protein fractions obtained from the infected Sf9 cells.

(A) Purification of rKLP61F. The following are shown: lane 1, Sf9 cell high-speed supernatant; lane 2, Ni-NTA affinity-column eluate; and lane 3, gel-filtration (Biogel A-15M, Biorad) fractionated and concentrated rKLP61F.

(B) Purification of rNcd. The following are shown: lane 1, Sf9 cell high-speed supernatant; lane 2, Ni-NTA affinity-column eluate; and lane 3, gel-filtration fractionated and concentrated Ncd.

(C) Purity of recombinant proteins eluted from gel-filtration columns as revealed by direct imaging of typical Coomassie-blue-stained SDS gels. Lane 1 shows rKLP61F, lane 2 shows rKLP61F T933E, and lane 3 shows rNcd.

KLP61F and Ncd, whether their interaction could control the speed and polarity of MT motility (and, by extrapolation, the rate of spindle elongation), and whether the antagonism between these motors could stall MT sliding in a manner capable of producing the predicted transient, stable steady-state spindle lengths observed in vivo [28, 32–34]. Such assays, performed with multiple KLP61F and Ncd motors, could also address how collective motor action influences MT motility [35]. With multiple low-duty-ratio kinesin-14 motors and even small numbers of high-duty-ratio kinesin-5 motors, it is unclear how each attached motor could take a step if others are attached in a different chemical state and not ready to take a step. It is possible that strain-dependent mechanochemistry must synchronize their mechanochemical cycles so that they all take a step at once [36–38]. Such collective action could cause complex motility—for example oscillations [36, 39].

Here, we investigated these issues with purified active KLP61F and Ncd. Specifically, we assayed KLP61F to identify a domain (lacking the bimC box) that is important for its homotetramerization and to investigate KLP61F interaction with Ncd in multiple-motor motility assays, with the aim of testing the feasibility of the predicted antagonistic-sliding-filament mechanism.

Results

Purification of Recombinant rKLP61F and rNcd

The yields of KLP61F purified from *Drosophila* embryos via MT affinity were too low for extensive biochemistry [2], and we were unable to purify Ncd from embryos because of its low abundance (next section). Ncd and KLP61F have been purified from bacterial expression systems [21, 23, 25, 40], but in our hands these preparations tended to aggregate and precipitate. Here, we

Table 1. Yields of rKLP61F and rNcd from 1 Liter Sf9 Cell Culture

	KLP61F Yield (mg)	Ncd Yield (mg)
Affinity (Ni-NTA) column	2.8	3.8
Gel-filtration column	0.9	1.5

used baculovirus expression to obtain high yields of monodisperse, purified, active, full-length rKLP61F and rNcd (Figure 1). Both proteins containing N-terminal 6× His-tags were purified from Sf9-cell high-speed supernatants with Ni-NTA affinity chromatography, followed by Biogel A-15M open-bed gel-filtration chromatography (yields ~0.9 mg pure rKLP61F and 1.5 mg rNcd per 1 liter culture; Table 1) and retained motility when stored on ice for up to 20 hr (in contrast to native KLP61F, which was inactivated within 6 hr [2]). We also expressed similar yields of a mutant KLP61F in which the phosphorylatable bimC box residue 933Thr was changed into Glu to mimic phospho-KLP61F (Figure 1C).

Oligomeric State of rKLP61F and rNcd

Native *Drosophila* embryo KLP61F is homotetrameric [2, 17] (Table 2). We estimated the oligomeric state of Ncd in embryo extracts by using immunoblotting of subfractions obtained with MT affinity, gel filtration, and sucrose-density-gradient centrifugation [2, 41] and found that its Stokes radius, sedimentation coefficient, and native molecular weight are consistent with a homodimeric structure (Table 2) similar to bacterially expressed Ncd [27]. Similarly, we measured the molecular weight (MW) of native purified baculovirus rKLP61F, the phosphomimic mutant KLP61F T933E, and rNcd, which are each composed of a single subunit on SDS gels (Figure 1C); these measurements were based on 5%–20% sucrose-gradient centrifugation and analytical gel-filtration fast-protein liquid chromatography (FPLC; superose 6 high-resolution [HR] 10/30, GE Pharmacia). The ratios of MW holoenzyme to MW subunits show that both wild-type and mutant rKLP61F are homotetramers, whereas rNcd is a homodimer (Table 2); the exact identity between the number of subunits per native and recombinant motor holoenzyme was a fortuitous surprise.

Identification of a KLP61F Homotetramerization Domain

The homotetrameric structure of kinesin-5 motors is thought to be essential for driving a MT-MT sliding-filament mechanism [19], but little is known about how it forms such a tetramer or whether the regulatory bimC box is required [22]. To identify sequences required for forming a KLP61F homotetramer, we analyzed oligomerization of KLP61F subfragments (Figure 2A).

Table 2. Comparison of Hydrodynamic Data between Native and Recombinant Proteins

	Native KLP61F	rKLP61F	rKLP61F T933E	Native Ncd	rNcd
Stokes radius (nm)	16.2	16.7	16.7	7.6	6.2
S value ($\times 10^{-13}$ s)	7.6	7.4	7.8	4.8	4.9
MW _{holo} (KD)	490.0	520.4	545.3	147.4	126.7
MW _{sub} (KD)	130.0	137.5	137.5	90.0	79.0
MW _{holo} /MW _{sub}	3.8	3.8	4.0	1.6	1.6

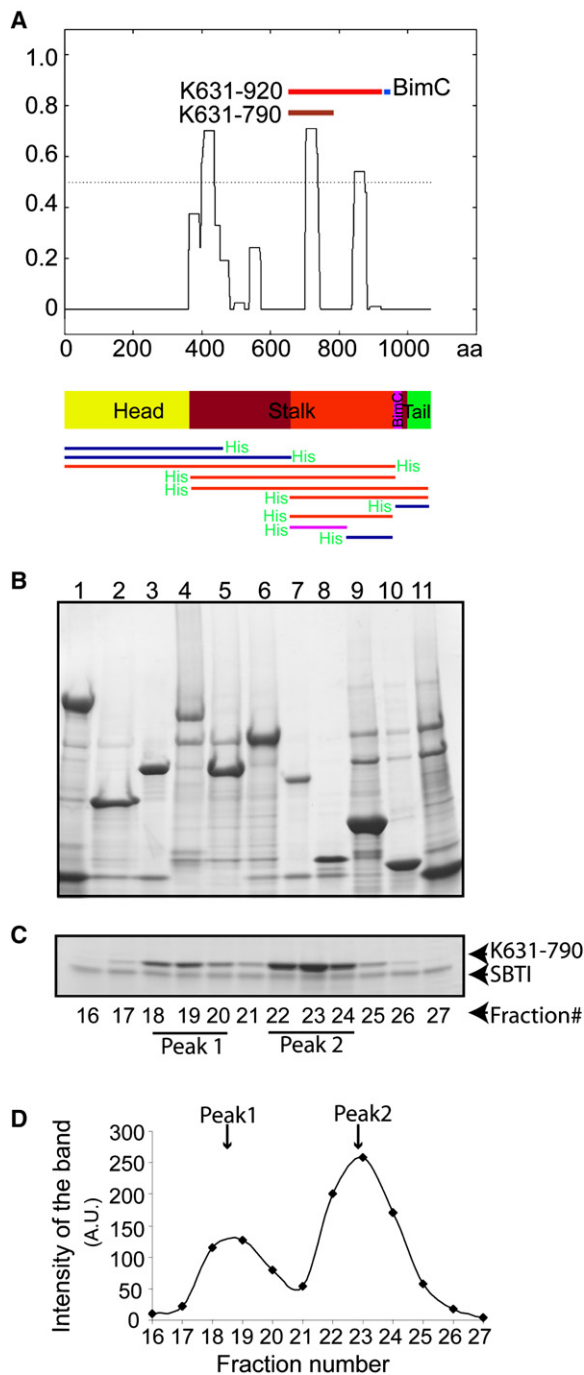


Figure 2. Purification of Different Fragments of KLP61F from the Baculovirus Expression System

(A) Predicted coiled-coil score based on KLP61F's amino acid sequence and the design of different fragments relative to the potential coiled-coil region. Green "His" stands for 6-histidine tag on the N or C terminus of the fragment.

(B) Coomassie-blue-stained 4%–20% gradient SDS-polyacrylamide gel of proteins eluted from Ni-NTA affinity columns. The following are shown: lane 1, full-length KLP61F; lane 2, fragment of KLP61F from residue 1 to residue 441 (K1-441); lane 3, fragment of KLP61F from residue 1 to residue 630 (K1-630); lane 4, fragment of KLP61F from residue 1 to residue 960 (K1-960); lane 5, fragment of KLP61F from residue 354 to residue 923 (K354-923); lane 6, fragment of KLP61F from residue 354 to residue 1066 (K354-1066); lane 7, fragment of KLP61F from residue 631 to residue 1066 (K631-1066); lane 8, fragment of KLP61F from residue 921 to residue 1066

Hydrodynamic analysis of baculovirus-expressed proteins (Figure 2B and Table 3) [2, 41] revealed that a region comprising the C-terminal half of the stalk domain (residues 631–920) is required for forming a stable tetramer. This region contains two predicted coiled coils. Interestingly, fragments lacking this region appeared to form monomers, whereas a subfragment of this domain (K631–790), which contains only the N-terminal coiled-coil segment, behaved as a mixture of dimer and tetramer in a molar ratio of 1.95:1.0 (Figures 2C and 2D). The K791–920 subfragment, which contains only the second predicted coiled coil, is a monomer. This suggests that the N-terminal coiled-coil region directs formation of an unstable tetramer, but the second coiled coil is required for tetramer stability. Significantly, the bimC-box and tail domains appear to have no effect on homotetramerization.

MT-Motility Assays

Purified baculovirus-expressed rKLP61F and rNcd move MTs in motility assays, as expected [2, 23, 25, 40]. rKLP61F is plus-end directed and moves MTs over coverslips with the minus ends (brighter part) leading at 0.04 $\mu\text{m/s}$, whereas rNcd is minus-end directed and moves MTs with the plus ends leading at 0.1 $\mu\text{m/s}$ (Figure 3A).

Full-Length, Motorless, and Tailless KLP61F Tetramers and Ncd Dimers Cross-link MTs into Bundles in MgATP

The antagonistic-sliding-filament model predicts that KLP61F and Ncd can cross-link MTs into bundles under physiological MgATP concentrations. To test this, we mixed pure full-length proteins (Figures 1A–1C) with fluorescent MTs in 1 mM ATP and examined them by fluorescence microscopy. This showed that KLP61F alone, Ncd alone, and mixtures of KLP61F and Ncd can bundle MTs under these conditions. However, a control dimeric kinesin-1 neck-motor-domain construct does not bundle MTs (Figure 3B), suggesting that MT cross-linking is not due to the action of two heads at only one end of the protein. Monomeric KLP61F subfragments and tetrameric-stalk subfragments lacking both the motor and C-terminal tail domains cannot cross-link MTs into bundles. Surprisingly, however, homotetrameric KLP61F subfragments containing either a head or a tail domain can bundle MTs (Table 3, Figure 3B), suggesting that both the head and tail domains of KLP61F can bind MTs in the presence of MgATP.

Cryo-electron microscopy confirmed that KLP61F and Ncd can bundle MTs. In the absence of either motor,

(K921-1066); lane 9, fragment of KLP61F from residue 631 to residue 920 (K631-920); lane 10, fragment of KLP61F from residue 631 to residue 790 (K631-790); and lane 11, fragment of KLP61F from residue 791 to residue 920 (K791-920).

(C) Coomassie-blue-stained 4%–20% gradient SDS-polyacrylamide gel of K631-790 fractions from analytical gel-filtration FPLC (superose 6 HR 10/30). Notice that the lower bands are the added protease inhibitor, soybean-trypsin inhibitor (SBTI).

(D) Intensity plots of scanned K631-790 bands from Coomassie-blue-stained SDS-polyacrylamide gels of the fractions (Figure 2C) show two peaks of fractions, from gel-filtration FPLC, corresponding to the K631-790 dimer and tetramer.

Table 3. Hydrodynamic and MT-Bundling Properties of Different-Length KLP61F Fragments

	Rs (nm)	S ($\times 10^{-13}$ s)	MWhole (KD)	MWsub (KD)	Ratio	Motility	Bundling Activity
rKLP61F full length	16.7	7.4	520.4	137.5	3.8	Yes	Yes
K1-441 head + neck	2.1	3.9	35.2	43.4	0.8	No	No
K1-630 head + 1/2 stalk	4.8	4.4	88.7	68.9	1.3	No	No
K1-960 head + stalk	16.4	6.3	437.0	106.3	4.1	Yes	Yes
K354-923 stalk-bimC	4.9	13.3	272.0	62.8	4.3	N/A	No
K354-1066 stalk + tail	16.4	5.5	377.7	91.5	4.1	N/A	Yes
K631-1066 1/2 stalk + tail	12.3	5.0	260.0	60.1	4.3	N/A	No
K921-1066 bimC + tail	2.7	2.6	29.5	25.8	1.1	N/A	No
K631-920 1/2 stalk	9.3	3.9	150.6	38.4	3.9	N/A	No
K631-790 1/4 stalk (peak 1)	5.5	3.5	81.4	21.0	3.9	N/A	No
K631-790 1/4 stalk (peak 2)	3.4	3.5	49.5	21.0	2.4	N/A	No
K791-920 1/4 stalk	2.8	2.3	26.4	19.0	1.4	N/A	No

individual MTs were observed to lie on the EM grid in random paths with no evidence of any interactions between adjacent MTs (Figures 4A, 4D, and 4G). However, upon incubation with KLP61F and/or Ncd under conditions identical to those used for fluorescence microscopy, the MTs were consistently organized into three-dimensional bundles that ranged in diameter from 50 to 1000 nm (Figures 4B, 4C, 4E, 4F, and 4H–J). It appeared that MT bundles formed by Ncd were more compact than those formed by KLP61F (Figures 4E and 4F), possibly because the shorter stalk of Ncd homodimers forms shorter MT-MT cross-bridges than those of the longer KLP61F stalk. Although indistinct protein molecules

decorated the MTs within these bundles, we were unable to clearly resolve the structure of the KLP61F and Ncd cross-bridges. In addition, although we consistently observed robust bundling by KLP61F and Ncd, we did not observe convincing MT-MT sliding in motility assays performed under these conditions, for which more sophisticated assays may be required [19].

Competitive-MT-Motility Assays

Our sliding-filament model suggests that KLP61F and Ncd function antagonistically to position spindle poles, but whether they can generate antagonistic forces to drive competitive motility has not been tested

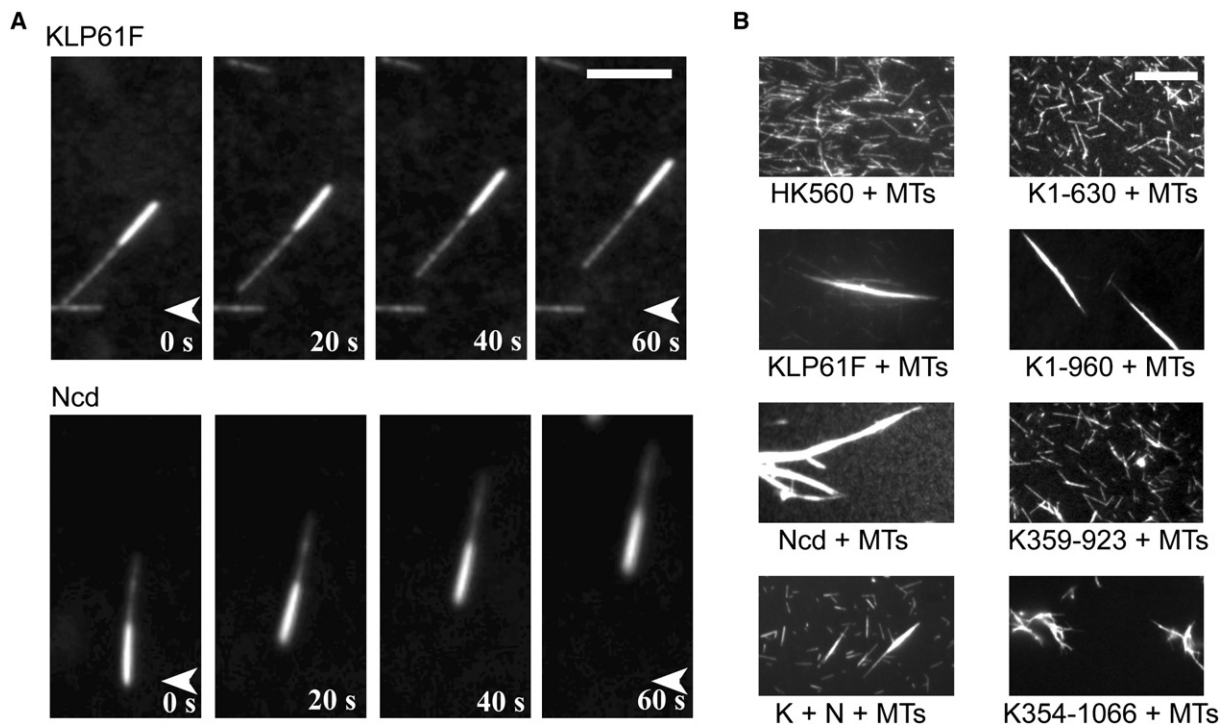


Figure 3. Purified rKLP61F and rNcd Can Move and Bundle MTs in 1m ATP

(A) MT gliding, driven by purified rKLP61F and rNcd, in motility assays. Polarity-marked MTs move in the gliding assays for rKLP61F and rNcd with velocities of 0.04 $\mu\text{m/s}$ and 0.10 $\mu\text{m/s}$, respectively. MT is minus-end leading in KLP61F gliding assay and is plus-end leading in Ncd gliding assay, which confirms that KLP61F is a plus-end-directed motor and Ncd is minus-end directed. The scale bar represents 5 μm .

(B) MT bundling by purified full-length rKLP61F, rNcd, and different fragments of KLP61F. Fluorescence microscopy shows that purified rKLP61F and rNcd have obvious bundling activity. In the presence of 1 mM ATP, free MTs cannot be bundled by HK560 but can form robust MT bundles in the presence of rKLP61F, rNcd, and rKLP61F + rNcd. Tetrameric K1-960 and K354-1066 can also form robust MT bundles at the same conditions. The scale bar represents 10 μm .

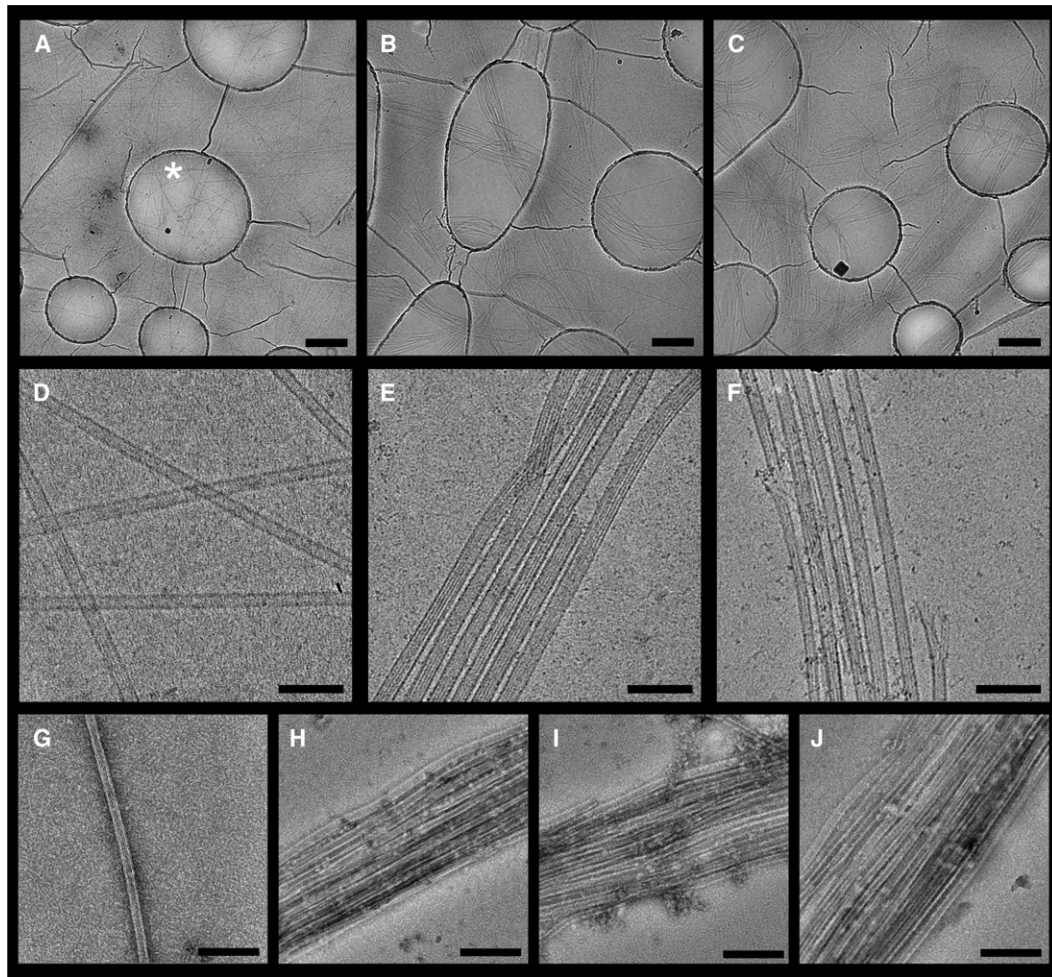


Figure 4. Electron-Micrograph Evidence for Microtubule Bundling by Purified KLP61F and Ncd

(A–C) Cryo-electron micrographs of microtubules vitrified on holey carbon film (A) alone, (B) incubated with Ncd, and (C) incubated with KLP61F. The vitrified sample layer covers the carbon film and spans the holes in the film (marked by * in [A]). The scale bars represent 1 μm .

(D–F) Higher-magnification cryo-electron micrographs of microtubules (D) alone, (E) incubated with Ncd, and (F) incubated with KLP61F. The scale bars represent 100 nm.

(G–J) Negative-stain micrographs of microtubules (G) alone, (H) incubated with Ncd, (I) incubated with KLP61F, and (J) incubated with KLP61F and Ncd. The scale bars represent 200 nm. Protein appears black in (A–F) and white in (G–J).

biochemically. To do so, we mixed KLP61F and Ncd in different molar ratios and monitored MT motility (Figure 5). In the presence of only Ncd (mole fraction of Ncd = 1.0), minus-end-directed motility at 0.1 $\mu\text{m}/\text{s}$ was observed, but as the mole fraction of Ncd decreased (i.e., increasing the relative concentration of KLP61F), the rate of Ncd-driven motility decreased in a dose-dependent manner (right part of Figure 5A). A similar but less-pronounced effect was seen when starting with only KLP61F and decreasing its relative concentration (left part of Figure 5A). At a certain “balance point” (mole fraction of Ncd = 0.7 on Figure 5A), MTs displayed a mean velocity of approximately zero. For brief time periods, the MTs lay immotile on the coverslip (e.g., 0–40 s in Figure 5B) but, although they never displayed persistent *net* motility in either the plus- or minus-end directions, they did display periods of oscillatory motion, rapidly switching back and forth between KLP61F-directed and Ncd-directed movement (e.g., 40–200 s in Figure 5B), at intermediate rates of 0.02 $\mu\text{m}/\text{s}$.

Quantitative Analysis of Competitive Motility Suggests that the KLP61F-Ncd Force Balance Determines the MT Sliding Rate

Using the method of [31] as described in the [Experimental Procedures](#), we estimate that there are $\sim 10^3$ motors per μm^2 surface of our assay chambers. Assuming that a MT fiber interacts with motors that are approximately ± 10 nm from its axis, we estimate that $\sim (10^3/\mu\text{m}^2) \times 20 \times 10^{-3} \mu\text{m} \approx 20/\mu\text{m}$ motors interact with MTs. Because MT lengths are between 3 and 6 μm , we estimate that ~ 100 motors interact with each MT in our assays (also see the theoretical estimate in the [Supplemental Data](#)). These numbers are plausibly similar to those acting on ipMTs in the spindle [12].

Without antagonism from KLP61F, multiple Ncd motors move MTs at approximately $-0.1 \mu\text{m}/\text{s}$, which is close to the rate of gliding of a single Ncd motor (we use positive values for the plus [KLP61F]-end-directed motors and negative values for the minus [Ncd]-end-directed motors). Similarly, without antagonism from

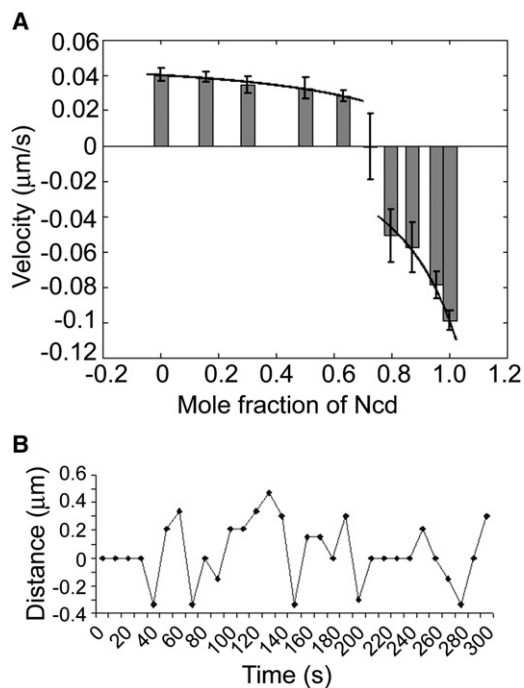


Figure 5. Antagonistic Motility Driven by Purified KLP61F and Ncd
(A) Plot of MT gliding velocities versus mole fraction of Ncd. The velocity is positive when MT motility is KLP61F directed and negative when MT motility is Ncd directed. The error bars represent the standard deviation of the velocity. The two black curves are the fits to the data from the mathematical model. Mole fraction refers to [(mol Ncd dimer)/(mol Ncd dimer + mol KLP61F tetramer)].
(B) Plot of displacements versus time for a typical MT at the “balance point.” The MT undergoes episodes of stationary behavior (e.g., 0–40 s) interspersed with episodes of oscillatory behavior (e.g., 40–220 s) during which positive KLP61F-driven excursions alternate with negative Ncd-driven excursions.

Ncd, multiple KLP61F motors move MTs at approximately $+0.04 \mu\text{m/s}$, close to the rate of gliding of a single kinesin-5 motor. Therefore, multiple Ncd or KLP61F motors can act in synchrony. However, in antagonistic-gliding assays (Figure 5), if the number of motors of one polarity is significantly greater than those of opposite polarity, then MTs are moved in the direction determined by the majority of motors, albeit with the average speed being a decreasing function of the fraction of the opposing motors. Specifically, when the mole fraction of KLP61F decreases from 1 to 0.4, the gliding rate decreases <2 -fold, from $0.04 \mu\text{m/s}$ to $\sim 0.025 \mu\text{m/s}$. On the other hand, when the mole fraction of Ncd decreases from 1 to 0.8, the gliding rate decreases >2 -fold, from $-0.1 \mu\text{m/sec}$ to approximately $-0.04 \mu\text{m/s}$. These data are consistent with the hypothesis that KLP61F is a strong, slow motor (i.e., with a relatively high stall force) that is slowed down relatively little by the faster, yet weak, Ncd motor, and vice versa. This is consistent with studies of kinesin-1 and dynein [31] and suggests that multiple opposite-polarity motors can generate unidirectional gliding of a single MT with speed and polarity determined by the balance between the relative numbers and strengths of antagonistic motors.

However, when we tried to fit the experimental mole-fraction-versus-velocity data (Figure 5) with a single formula for a force balance between two kinds of motors,

each characterized by its own certain force-velocity relationship, the fit worked only with strong nonlinearities in the force-velocity relations, and such nonlinearities are difficult to justify biologically. On the other hand, the data can be fit very simply if we assume that there are two qualitatively different regimes for plus-end- and minus-end-directed MT gliding, whereupon the corresponding quantitative model fits the data very well (Box 1; Figure 5).

The Onset of Directional Instability of MT Gliding When Opposing Motors Balance Each Other

It would be natural to expect that at a certain ratio of opposing motors, the motors would simply stall each other, so that MT gliding is not seen, but instead we found that gliding is not completely stalled in the narrow range of mole fractions ($\sim 28\%$ of KLP61F and $\sim 72\%$ of Ncd plus/minus several percent) in which net unidirectional MT gliding ceases. Rather, small MT oscillations occur so that MTs move bidirectionally by making short, irregular excursions alternately in the plus- and minus-end directions with rates of $\sim 0.02 \mu\text{m/s}$ (Figure 5), a behavior that is somewhat reminiscent of directional instability. The average duration and distance of MT excursions between the switches in the direction of movement are ~ 15 s and $\sim 0.3 \mu\text{m}$, respectively (Supplemental Data). The simplest explanation for the observed directional instability would be random power strokes by individual motors displacing a MT by a few nm at a time in either direction with equal probability, but quantitative analysis of the MT trajectories does not support this (Figure 5 and Supplemental Data), suggesting that other explanations must apply (see Discussion).

Discussion

Using purified, monodisperse, active homotetrameric KLP61F and homodimeric Ncd, we demonstrated that both of these motors can cross-link MTs into bundles in MgATP and showed that they drive antagonistic MT sliding in motility assays. We also found that the C-terminal half of the rod is essential for homotetramer assembly by KLP61F and is required for the MT-MT cross-linking that underlies its postulated sliding-filament mechanism. Quantitative analysis suggests that antagonistic sliding could control the rate of spindle elongation and could produce a steady-state prometaphase spindle length, but with individual interpolar MTs undergoing small bidirectional movements.

Homotetramerization of KLP61F and the Sliding-Filament Mechanism

Although kinesin-5 motors very likely form bipolar homotetramers with motor domains on opposite ends of a rod [2, 17–19], little is known about the structural determinants required. The finding that the phosphorylation of the bimC box in the tail domain of kinesin-5 targets this motor to mitotic-spindle MTs [22], where it could slide apart ipMTs to push apart the spindle poles [21], suggested that the bimC box could activate homotetramerization. However, a stalk segment (residues 631–920) that lacks the bimC box can form homotetramers. This, together with the observation that a bimC-box

Box 1. Force Balance Model of KLP61F-Ncd Action

We make the following assumptions:

- (1) First, both Ncd and KLP61F are characterized by linear force-velocity relations: One motor generates the force $f = f_{n,k}(1 \pm \frac{v}{V_{n,k}})$, where indices n and k correspond to Ncd and KLP61F, respectively. Here, v is the gliding rate, $f_{n,k}$ is the maximal force generated at stall, and $V_{n,k}$ is the free-motor gliding rate in the absence of the load. Such relation is a good approximation for mechanical properties of Eg5, analog of KLP61F [B1]; we assume it is qualitatively similar for Ncd.
- (2) Second, the net force generated by a number of synchronized motors is additive: n Ncd motors generate force $nf_n(1 + \frac{v}{V_n})$, and k KLP61F motors generate force $kf_k(1 - \frac{v}{V_k})$.
- (3) Third, a smaller number of opposing motors are unable to complete their power strokes when pulled against their natural direction (as observed for the kinesin-5, Eg5 [B1], and assumed for Ncd). Instead, the opposing motors work as “brakes,” exerting effective protein friction and slowing down the “winning majority” of motors. This force is proportional to the sliding rate [B2]. Strong KLP61F motors become a brake if there are fewer than ~25% of them; then they exert the resistive force $k\zeta_k v$, where ζ_k is the corresponding effective-drag coefficient for one KLP61F motor. Similarly, weak Ncd motors become a brake if there are fewer than ~65% of them; then

they exert the resistive force $n\zeta_n v$, where ζ_n is the corresponding effective-drag coefficient for one Ncd motor.

The resulting two equations, $nf_n(1 + \frac{v}{V_n}) = k\zeta_k v$ and $kf_k(1 - \frac{v}{V_k}) = n\zeta_n v$, which correspond to two opposite directions of MT gliding, can be solved analytically (Supplemental Data). The solutions express the gliding rates as functions of the Ncd molar fraction:

$$v = \begin{cases} \frac{V_n x}{x + \varepsilon_k(1-x)}, \varepsilon_k = \frac{\zeta_k V_n}{f_n} & \text{if } x > 0.75 \\ \frac{V_k(1-x)}{(1-x) + \varepsilon_n x}, \varepsilon_n = \frac{\zeta_n V_k}{f_k} & \text{if } x < 0.65 \end{cases}$$

where $x = \frac{n}{n+k}$ is the Ncd molar fraction and ε_k and ε_n are the normalized protein-friction drag coefficients. Note that the result depends on two known free-gliding motor velocities and only two unknown parameters, ε_k and ε_n . These parameters can be found by fitting the data (Supplemental Data).

Box References

- B1. Valentine, M.T., Fordyce, P.M., Krzysiak, T.C., Gilbert, S.P., and Block, S.M. (2006). Individual dimers of the mitotic kinesin motor Eg5 step processively and support substantial loads in vitro. *Nat. Cell Biol.* 8, 470–476.
- B2. Tawada, K., and Sekimoto, K. (1991). Protein friction exerted by motor enzymes through a weak-binding interaction. *J. Theor. Biol.* 150, 193–200.

phosphomimic mutant can form homotetramers just like nonphosphorylated KLP61F, suggests that the bimC box does not participate in tetramer formation.

Instead, we identified within the stalk segment an assembly domain (K631-920) that contains two predicted coiled-coil regions. Fragments lacking this domain form monomers, whereas fragments containing it form tetramers of different stability. Of the two coiled coils within K631-920, the N-terminal coiled coil located within subfragment K631-790 directs formation of dimers and tetramers, whereas the C-terminal coiled coil located within subfragment K791-920 directs monomer formation. These results suggest that the entire region spanning residues 631 to 920 is required to form stable tetramers.

The idea that homotetramers are required for a KLP61F-driven sliding-filament mechanism [2, 17–19, 21] is supported by the demonstration that KLP61F, like Ncd [25], is capable of forming robust MT-MT bundles in MgATP. Significantly, full-length, motorless, and tailless tetramers, but not monomers or tetramers lacking both the motor and tail domains, could bundle MTs, suggesting that both the motor and tail domains have MT binding activity. However, in our assays, we did not obtain convincing evidence for MT-MT sliding. While our work was in progress [19], elegant optical-trap experiments demonstrated that frog kinesin-5 can

indeed slide apart MTs in vitro, providing support for the sliding-filament mechanism. It seems plausible that similar biophysical approaches would reveal that KLP61F is capable of driving such motility.

Antagonistic MT Motility Driven by KLP61F and Ncd

Using competitive-MT-motility assays, we showed that multiple KLP61F and Ncd motors can act synchronously to antagonize one another. The assays demonstrate that when these motors act collectively, KLP61F motors are strong and slow, whereas Ncd motors are weak and fast, in agreement with [20, 26, 29]. Motors of the same polarity are able to cooperate, even in the presence of a small number of opposite-polarity motors. The opposing motors are unable to generate power strokes but rather act as brakes by attaching and detaching from MTs and generating protein friction. This has important biological implications for the mitotic spindle, where multiple motors of opposite polarity act on pairs of overlapping MTs and compete mechanically. Our in vitro assay justifies models suggesting that by regulating relative numbers and activities of the opposite-polarity motors, the cell can regulate the rates of spindle elongation [33, 34]. Furthermore, our model predicts that motorless KLP61F constructs would cross-link MTs to provide drag at all mole fractions, but not motility, causing the curved region of the velocity–mole-fraction

relation, a region corresponding to active Ncd in Figure 5, to now extend to the whole range of the mole fractions.

We also made an important observation that in order to stall MT sliding, the ratios of the opposite-polarity motors have to be fine tuned in a very narrow range, and even when the motors balance each other, true mechanical equilibrium is not achieved. This is contrary to expectations from earlier work [31], in which the authors speculated that the directional-instability regime is characteristic for a small number of motors associated with each individual MT and that a large number of balanced opposing motors (as in our study) would truly stall gliding. Rather than stalling one another to produce immotile MTs, multiple balanced opposite-polarity motors exhibit very small fluctuations, reminiscent of directional instability, by switching between short periods of partial synchronization of the same type of motors. This directional-instability regime is not similar to that observed during prometaphase when chromosomes make more persistent poleward and antipoleward excursions with more or less constant speed [42]. In that case, the corresponding velocity distribution is strongly bipolar, whereas in our assay, the MT velocity is normally distributed with the mean zero and standard deviation of $\sim 0.02 \mu\text{m/s}$, so that the MT is usually either pausing or moving slowly (Supplemental Data).

What is the explanation? Monastrol-inhibited kinesin-5 displays diffusive motion with a similar effective-diffusion coefficient ($\sim 1000\text{--}3000 \text{ nm}^2/\text{s}$) to that of the directionally unstable MTs observed over long time scales in our study ([43] and Supplemental Data). Thus, it is possible that balanced, mitotic motors move diffusively to produce random runs in both directions. However, the multiple motors would have to synchronize the directions of these runs, but the mechanism of such synchronization is unclear. It is also possible that MTs glide on a spatially varying landscape, created by stochastic variations in the local surface density of KLP61F and Ncd, so that periods of unidirectional gliding are due to patches where one type of motor dominates, and reversals are due to lateral MT movements from one patch to another. Finally, it could be that when the antagonistic motors are almost balanced, one kind of motor “wins,” but only transiently, because the opposing load is too strong, increasing the effective dissociation rate of the winning motors so the number of working winning motors exponentially decreases. When almost all the winning motors dissociate, after a brief pause, either motor makes a stochastic synchronous step to start a new unidirectional run. Repeated, this cycle would result in the observed bidirectional gliding. Further work will be needed to elucidate the microscopic mechanism of the directional instability.

Implications for Mitotic-Spindle Assembly and Elongation in *Drosophila* Embryos

The results show that KLP61F and Ncd can drive antagonistic MT motility, which we propose may be important in maintaining spindle length specifically at the onset of the prometaphase-metaphase transition in *Drosophila* embryos [9, 10]. However, other factors clearly play important roles in spindle-length determination as well. For example, in embryonic spindles at subsequent metaphase, the KLP61F-dependent outward sliding of the

ipMTs is counterbalanced by their depolymerization at the poles, leading to a constant spindle length, whereas the suppression of depolymerization leads to anaphase B spindle elongation [11, 12]. Moreover, there are suggestions that these and other mitotic motors are deployed differently in S2 cells [44], as reflected in observations that loss of Ncd function by RNAi in S2 cells causes severe disorganization of spindle poles [45], whereas in *ncd* null embryos, spindle poles remain focused and only minor truncations of the extent of the prometaphase and metaphase steady state are observed [11]. Further work will be required to determine exactly how the proposed KLP61F-Ncd antagonistic-sliding-filament mechanism is deployed in different situations.

Motility assays combined with quantitative modeling are consistent with the hypothesis that KLP61F and Ncd motors serve as brakes to slow down one another's activity. It is plausible to think that during mitosis, the resulting force balance may be regulated so as to modulate the number of active KLP61F and Ncd motors, and this regulation could in turn control the rate and extent of spindle-pole separation as has been proposed for the control of the rate of mitotic movements at different stages of mitosis, on the basis of *in vivo* studies and modeling [10, 28, 33]. However, at the balance point, the two motors do not completely stall one another to produce immotile MTs as would be predicted if the KLP61F-Ncd force balance, acting on its own, were to maintain a completely stable steady-state prometaphase spindle length, as in the transient-steady-state model for spindle assembly [9, 10]. Instead, at the balance point, MTs can remain immotile for periods of tens of seconds, but they also undergo episodes of unstable, oscillatory behavior, moving alternately over submicrometer distances in the plus- and minus-end directions at a rate intermediate between the rate of KLP61F or Ncd alone. Despite these small fluctuations, it is possible that KLP61F and Ncd can maintain a stable prometaphase spindle length of the type observed in *Drosophila* embryos because (1) such fluctuations are too small to be detected by light-microscopic observations of pole-pole spacing *in vivo*, and (2) in the spindle, many mechanically coupled interpolar MTs cooperate to regulate spindle length, and the concerted action of these multiple MTs, undergoing nonsynchronous small fluctuations, would cancel out the fluctuations displayed by individual MTs of the type observed in our *in vitro* assays. Finally, it is also possible that other factors, for example the buffering of ipMT sliding by MT depolymerases on the spindle poles [11, 12, 44] or unusual hetero-oligomeric arrays [32], may contribute to the maintenance of the steady-state length of the mitotic spindle.

Experimental Procedures

Motility Assays

Polarity-marked MT gliding over a casein-treated glass coverslip coated with pure rKLP61F or pure rNcd was performed as described previously [2], with a few modifications. We used buffer L (20 mM Tris [pH 8.0], 75 mM KCl, 2 mM MgCl_2 , 2 mM DTT, protease inhibitors) to replace PMEG buffer (100 mM K_2PIPES [pH 6.9], 5 mM EGTA, 0.5 mM EDTA 2.5 mM MgSO_4 , 0.9 M glycerol, 1 mM DTT, protease inhibitors) because rKLP61F and rNcd were precipitated in PMEG. Polarity-marked MTs were seen by fluorescence microscopy

to glide over the coverslip surface in the presence of 1 mM ATP. Images were taken and analyzed with Metamorph Imaging software (Universal Image). For antagonistic-sliding assays, both pure rKLP61F and rNcd were used right after the gel-filtration column without freezing. The adsorption efficiency of the motor protein to the coverslip was determined by using the bioassay described by Ron Vale [31]. Within the assay's concentration range, KLP61F, Ncd, and KLP61F mixed with Ncd display essentially 100% adsorption to the casein-coated surfaces. Different ratios of rKLP61F and rNcd were mixed and then applied into the flow cells for the gliding assay. Assays of different ratios of motors were performed with the same batches of purified proteins. Serial dilutions of the motor protein to find the minimal required concentration for motility was used as a standard to ensure that each protein keeps the same "active concentration" through the whole assay. Only MTs performing smooth movements (no pauses or collisions with other MTs) for more than 1 min (except at the balance point) were used for velocity measurements.

MT-Bundling Assays

For full-length rKLP61F and rNcd, the gel-filtration fractions were pooled and concentrated by Centrprep 30 as described previously [2]. For different KLP61F fragments, the proteins purified from Ni-NTA affinity columns were dialyzed against buffer L, and the samples were then centrifuged at 12,000 × g for 15 min to remove any protein aggregates. Fluorescent MTs were polymerized by incubating 25 μM tubulin (Cytoskeleton) + 1 μM rhodamine tubulin (Cytoskeleton) with 1 mM GTP and 10 μM taxol in BRB80 (80 mM K₂PIPES, 1 mM EGTA, 1 mM MgCl₂) + 10% glycerol at 37°C for 35 min. MTs were pelleted and resuspended in buffer L. Bundling assays were performed in buffer L with 2.5 μM MTs, 0.2 μM motor proteins or fragments thereof, 10 μM taxol, and 1 mM ATP (final concentrations). The mixture was rocked at room temperature for 30 min. Mixtures of 25 μl were transferred into a flow chamber with a 0.02 mg/ml DEAE-Dextran-coated coverslip. The unstuck mixture was washed out with 75 μl buffer L + 1 mM ATP + 10 μM taxol + antifade after 3 min. Bundling of fluorescent MTs was observed by fluorescence microscopy (Nikon E600). Human kinesin-1, fragment HK560 (1–560 aa with GFP on the C terminus) was a gift from Ron Vale's Lab at UCSF and was used under the same conditions as a control. Each experiment was repeated more than three times to ensure consistent results.

Supplemental Data

Supplemental Data include a discussion of theory, Experimental Procedures, and three figures and are available with this article online at: <http://www.current-biology.com/cgi/content/full/16/23/2293/DC1/>.

Acknowledgments

We thank Dr. Ron Vale for HK560 construct. We thank Dr. Frank McNally, Dr. Bo Liu, and Dr. Ingrid Brust-Mascher for discussion and anonymous reviewers for useful suggestions. This work was supported by National Institutes of Health (NIH) grants GM 55507 to J.M.S. and GM 068952 to A.M and J.M.S.

Received: July 30, 2006

Revised: September 26, 2006

Accepted: September 27, 2006

Published: December 4, 2006

References

- Lawrence, C.J., Dawe, R.K., Christie, K.R., Cleveland, D.W., Dawson, S.C., Endow, S.A., Goldstein, L.S., Goodson, H.V., Hirokawa, N., Howard, J., et al. (2004). A standardized kinesin nomenclature. *J. Cell Biol.* 167, 19–22.
- Cole, D.G., Saxton, W.M., Sheehan, K.B., and Scholey, J.M. (1994). A "slow" homotetrameric kinesin-related motor protein purified from *Drosophila* embryos. *J. Biol. Chem.* 269, 22913–22916.
- Cottingham, F.R., Gheber, L., Miller, D.L., and Hoyt, M.A. (1999). Novel roles for *Saccharomyces cerevisiae* mitotic spindle motors. *J. Cell Biol.* 147, 335–350.
- Enos, A.P., and Morris, N.R. (1990). Mutation of a gene that encodes a kinesin-like protein blocks nuclear division in *A. nidulans*. *Cell* 60, 1019–1027.
- Heck, M.M., Pereira, A., Pesavento, P., Yannoni, Y., Spradling, A.C., and Goldstein, L.S. (1993). The kinesin-like protein KLP61F is essential for mitosis in *Drosophila*. *J. Cell Biol.* 123, 665–679.
- Saunders, W.S., and Hoyt, M.A. (1992). Kinesin-related proteins required for structural integrity of the mitotic spindle. *Cell* 70, 451–458.
- Sawin, K.E., LeGuellec, K., Philippe, M., and Mitchison, T.J. (1992). Mitotic spindle organization by a plus-end-directed microtubule motor. *Nature* 359, 540–543.
- Straight, A.F., Sedat, J.W., and Murray, A.W. (1998). Time-lapse microscopy reveals unique roles for kinesins during anaphase in budding yeast. *J. Cell Biol.* 143, 687–694.
- Sharp, D.J., Yu, K.R., Sisson, J.C., Sullivan, W., and Scholey, J.M. (1999). Antagonistic microtubule-sliding motors position mitotic centrosomes in *Drosophila* early embryos. *Nat. Cell Biol.* 1, 51–54.
- Sharp, D.J., Brown, H.M., Kwon, M., Rogers, G.C., Holland, G., and Scholey, J.M. (2000). Functional coordination of three mitotic motors in *Drosophila* embryos. *Mol. Biol. Cell* 11, 241–253.
- Brust-Mascher, I., and Scholey, J.M. (2002). Microtubule flux and sliding in mitotic spindles of *Drosophila* embryos. *Mol. Biol. Cell* 13, 3967–3975.
- Brust-Mascher, I., Civelekoglu-Scholey, G., Kwon, M., Mogilner, A., and Scholey, J.M. (2004). Model for anaphase B: Role of three mitotic motors in a switch from poleward flux to spindle elongation. *Proc. Natl. Acad. Sci. USA* 101, 15938–15943.
- Kwok, B.H., Yang, J.G., and Kapoor, T.M. (2004). The rate of bipolar spindle assembly depends on the microtubule-gliding velocity of the mitotic kinesin Eg5. *Curr. Biol.* 14, 1783–1788.
- Miyamoto, D.T., Perlman, Z.E., Burbank, K.S., Groen, A.C., and Mitchison, T.J. (2004). The kinesin Eg5 drives poleward microtubule flux in *Xenopus laevis* egg extract spindles. *J. Cell Biol.* 167, 813–818.
- Shirasu-Hiza, M., Perlman, Z.E., Wittmann, T., Karsenti, E., and Mitchison, T.J. (2004). Eg5 causes elongation of meiotic spindles when flux-associated microtubule depolymerization is blocked. *Curr. Biol.* 14, 1941–1945.
- Kashina, A.S., Scholey, J.M., Leszyk, J.D., and Saxton, W.M. (1996). An essential bipolar mitotic motor. *Nature* 384, 225.
- Kashina, A.S., Baskin, R.J., Cole, D.G., Wedaman, K.P., Saxton, W.M., and Scholey, J.M. (1996). A bipolar kinesin. *Nature* 379, 270–272.
- Gordon, D.M., and Roof, D.M. (1999). The kinesin-related protein Kip1p of *Saccharomyces cerevisiae* is bipolar. *J. Biol. Chem.* 274, 28779–28786.
- Kapitein, L.C., Peterman, E.J., Kwok, B.H., Kim, J.H., Kapoor, T.M., and Schmidt, C.F. (2005). The bipolar mitotic kinesin Eg5 moves on both microtubules that it crosslinks. *Nature* 435, 114–118.
- Valentine, M.T., Fordyce, P.M., Krzysiak, T.C., Gilbert, S.P., and Block, S.M. (2006). Individual dimers of the mitotic kinesin motor Eg5 step processively and support substantial loads in vitro. *Nat. Cell Biol.* 8, 470–476.
- Sharp, D.J., McDonald, K.L., Brown, H.M., Matthies, H.J., Walczak, C., Vale, R.D., Mitchison, T.J., and Scholey, J.M. (1999). The bipolar kinesin, KLP61F, cross-links microtubules within inter-polar microtubule bundles of *Drosophila* embryonic mitotic spindles. *J. Cell Biol.* 144, 125–138.
- Sawin, K.E., and Mitchison, T.J. (1995). Mutations in the kinesin-like protein Eg5 disrupting localization to the mitotic spindle. *Proc. Natl. Acad. Sci. USA* 92, 4289–4293.
- Walker, R.A., Salmon, E.D., and Endow, S.A. (1990). The *Drosophila* claret segregation protein is a minus-end directed motor molecule. *Nature* 347, 780–782.
- Meluh, P.B., and Rose, M.D. (1990). KAR3, a kinesin-related gene required for yeast nuclear fusion. *Cell* 60, 1029–1041.

25. McDonald, H.B., Stewart, R.J., and Goldstein, L.S. (1990). The kinesin-like *ncd* protein of *Drosophila* is a minus end-directed microtubule motor. *Cell* 63, 1159–1165.
26. Endres, N.F., Yoshioka, C., Milligan, R.A., and Vale, R.D. (2006). A lever-arm rotation drives motility of the minus-end-directed kinesin *Ncd*. *Nature* 439, 875–878.
27. Chandra, R., Salmon, E.D., Erickson, H.P., Lockhart, A., and Endow, S.A. (1993). Structural and functional domains of the *Drosophila ncd* microtubule motor protein. *J. Biol. Chem.* 268, 9005–9013.
28. Sharp, D.J., Rogers, G.C., and Scholey, J.M. (2000). Microtubule motors in mitosis. *Nature* 407, 41–47.
29. deCastro, M.J., Fondacave, R.M., Clarke, L.A., Schmidt, C.F., and Stewart, R.J. (2000). Working strokes by single molecules of the kinesin-related microtubule motor *ncd*. *Nat. Cell Biol.* 2, 724–729.
30. Stewart, R.J., Semerjian, J., and Schmidt, C.F. (1998). Highly processive motility is not a general feature of the kinesins. *Eur. Biophys. J.* 27, 353–360.
31. Vale, R.D., Malik, F., and Brown, D. (1992). Directional instability of microtubule transport in the presence of kinesin and dynein, two opposite polarity motor proteins. *J. Cell Biol.* 119, 1589–1596.
32. Nedelec, F. (2002). Computer simulations reveal motor properties generating stable antiparallel microtubule interactions. *J. Cell Biol.* 158, 1005–1015.
33. Cytrynbaum, E.N., Scholey, J.M., and Mogilner, A. (2003). A force balance model of early spindle pole separation in *Drosophila* embryos. *Biophys. J.* 84, 757–769.
34. Cytrynbaum, E.N., Sommi, P., Brust-Mascher, I., Scholey, J.M., and Mogilner, A. (2005). Early spindle assembly in *Drosophila* embryos: Role of a force balance involving cytoskeletal dynamics and nuclear mechanics. *Mol. Biol. Cell.* 16, 4967–4981.
35. Vermeulen, K.C., Stienen, G.J., and Schmid, C.F. (2002). Cooperative behavior of molecular motors. *J. Muscle Res. Cell Motil.* 23, 71–79.
36. Badoual, M., Julicher, F., and Prost, J. (2002). Bidirectional cooperative motion of molecular motors. *Proc. Natl. Acad. Sci. USA* 99, 6696–6701.
37. Julicher, F., and Prost, J. (1995). Cooperative molecular motors. *Phys. Rev. Lett.* 75, 2618–2621.
38. Duke, T. (2000). Cooperativity of myosin molecules through strain-dependent chemistry. *Philos. Trans. R. Soc. Lond. B Biol. Sci.* 355, 529–538.
39. Shingyoji, C., Higuchi, H., Yoshimura, M., Katayama, E., and Yanagida, T. (1998). Dynein arms are oscillating force generators. *Nature* 393, 711–714.
40. Barton, N.R., Pereira, A.J., and Goldstein, L.S. (1995). Motor activity and mitotic spindle localization of the *Drosophila* kinesin-like protein KLP61F. *Mol. Biol. Cell* 6, 1563–1574.
41. Siegel, L.M., and Monty, K.J. (1966). Determination of molecular weights and frictional ratios of proteins in impure systems by use of gel filtration and density gradient centrifugation. Application to crude preparations of sulfite and hydroxylamine reductases. *Biochim. Biophys. Acta* 112, 346–362.
42. Skibbens, R.V., Skeen, V.P., and Salmon, E.D. (1993). Directional instability of kinetochore motility during chromosome congression and segregation in mitotic newt lung cells: A push-pull mechanism. *J. Cell Biol.* 122, 859–875.
43. Kwok, B.H., Kapitein, L.C., Kim, J.H., Peterman, E.J., Schmidt, C.F., and Kapoor, T.M. (2006). Allosteric inhibition of kinesin-5 modulates its processive directional motility. *Nat. Chem. Biol.* 2, 480–485.
44. Goshima, G., Wollman, R., Stuurman, N., Scholey, J.M., and Vale, R.D. (2005). Length control of the metaphase spindle. *Curr. Biol.* 15, 1979–1988.
45. Morales-Mulia, S., and Scholey, J.M. (2005). Spindle pole organization in *Drosophila* S2 cells by dynein, abnormal spindle protein (Asp), and KLP10A. *Mol. Biol. Cell* 16, 3176–3186.